Regular Article

PHYSICAL CHEMISTRY RESEARCH
Published by the
Iranian Chemical Society
www.physchemres.org
info@physchemres.org

Phys. Chem. Res., Vol. 1, No. 2, 166-174, December 2013.

Quantum Dots of CdS Synthesized by Micro-Emulsion under Ultrasound: Size Distribution and Growth Kinetics

N. Ghows and M.H. Entezari*

Department of Chemistry, Ferdowsi University of Mashhad, 91775, Mashhad, Iran

(Received 7 May 2013, Accepted 29 August 2013)

Quantum dots of CdS with hexagonal phase were prepared at relatively low temperature and short time compared to the other methods reported in the literature by micro-emulsion (O/W) under ultrasound. This study was focused on the particle size distribution and the growth kinetics. The particle size distribution obtained from the optical absorption edge. It was relatively symmetrical with sonication time. In addition, an agreement was observed with the size distribution obtained from the TEM images of the sample under ultrasound. The growth kinetics was monitored by the red-shift in UV-Visible absorbance peaks. The cubed average particle radius showed an emergence of linear regions at longer times. This indicates that the increase of particle size at longer time can be attributed to the diffusion-limited coarsening process. The rate constant for the coarsening increases with increasing the temperature. The Arrhenius-type plot was created by using the slopes of Lifshitz-Slyozov-Wagner (LSW) curves. The activation energy was 71.72 kJ mol^{-1} for the ripening process. In fact, the acoustic cavitation strongly increases the diffusion of surface atoms.

Keywords: Quantum dots, Microemulsion, CdS, Ultrasound, Coarsening, particle size distribution

INTRODUCTION

Semiconductor quantum dots (QDs) have been widely studied in recent years owing to their size dependent properties and the wide range of potential applications [1-3]. Among the II–VI semiconductors, CdS is a fascinating material with ideal band gap energy (2.4 eV). Various techniques have been successfully developed for the synthesis of CdS nano-crystals. The important methods used are electrochemical methods [4], gamma-irradiation [5], solvo-hydrothermal [6], thermal evaporation [7], microwave [8], microemulsion[9] and ultrasonic method [10].

Among different methods, the preparation of uniform nanoparticles with ultrasound is easy and more effective under mild conditions [11-14]. During the irradiation of liquids with ultrasound, the extreme and transient local conditions caused by acoustic cavitation (5000 K, 500 bar) [15] not only decompose organometallic precursors to form nanometer-sized inorganic particles [16-18], but also facilitate the crystallization of the semiconductors [19,20].

*Corresponding author. E-mail: moh_entezari@yahoo.com

Additionally, acoustic cavitation produced by ultrasonic waves can strongly increase the surface area and the mass transfer between the two phases [21,22]. Our recent works confirmed that the synthesis of nanocrystal is easier with ultrasound than other methods [23,24]. These works also showed that the combination of ultrasound and micro-emulsion is suitable for the synthesis of CdS nano-particles and this combination is useful for controlling crystal phase, morphology, and the size of the nano-particles. The electrical and optical properties of semiconductor nano-crystals are often size dependent. In semiconductors with very small size, quantum confinement modulates the band structure of nano-particles and increases the band gap [25,26]. The control of nanoparticles' properties is significant for many technological applications such as light-emitting diodes [27], biological labels [28], lasers [29], and microcavities [30]. Hence, it is essential to understand the details of nucleation and growth and how they influence the evolution of the particle size [2,26,31-34]. The particle size is dependent on the kinetics of nucleation and growth from a supersaturated solution as well as processes such as coarsening [35,36,26], oriented attachment [37,38] and

aggregation. In synthesis inside the solution, processes such as coarsening and aggregation can compete with nucleation and growth in modifying the particle size distribution in the system. A detailed understanding of the growth behavior of these systems is essential for the control of particle sizes and hence optical properties.

Despite many reports on the synthesis and characterization of quantum size particles, there are relatively few reports on the growth kinetics of these kinds of particles. Searson *et al.* reported the detail ripening kinetics of nanocrystals such as ZnO, TiO_2, CdSe, *etc.* [26,33,34,39-42] and they used Lifshitz-Slyozov-Wagner (LSW) theory [35,36] for the ripening kinetics of the nanocrystals. The same work was observed by Sung *et al.* [2]. Also, Searson *et al.* reported the relationship between absorbance spectra and particle size distributions for quantum-sized nanocrystals [26,34,43]. Yadav *et al.* confirm the growth of nanoparticles occurs *via* two processes with the deviation in the linear relation in between cube of radius and time of ultrasonic irradiation (diffusion process and the reaction at the surface) [44].

There is relatively rare reports on the growth process under ultrasound [44]. To the best of our knowledge, no detailed studies of the growth process under ultrasound has been reported by the particle size distribution obtained from the optical absorption edge. The shape of the absorbance edge of semicounductor quantum dots is influenced by the electronic transition and the distribution of band gaps. In this paper, this relationship has been confirmed by comparing the particle size distribution obtained from analysis of the absorption edge with the size distribution obtained from analysis of TEM images in the presence of ultrasound. In this paper it is shown that the growth of the CdS particles under ultrasound is diffusion-dependent and follows Ostwald ripening kinetics according to LSW theory. The time and temperature dependence of the primary particle size are analyzed quantitatively and calculated the activation energy.

EXPERIMENTAL

Materials

Ethylenediamine, sulfur, p-xylen, CTAB and 1-butanol from Merck and $CdCl_2$, $2H_2O$ from Fluka have been used without further purification. De-ionized water was used for the sample preparation.

Procedure

Synthesis of nanoparticles. The synthesis of nanoparticles has been done in our laboratory through the combination of ultrasound and microemulsion [23]. First, 1000 mg of sulfur was dissolved in 50 ml of p-xylen at about 313 K. Then, a quaternary oil-in-water micro-emulsion formed by CTAB/1-butanol/p-xylen/water (3.310%, 6.610%, 1.978%, 88.102%) with an aprppriate ratio was used as a reaction medium for CdS nano-particles preparation. The composite of micro-emulsion was set with weight ratio between oil and CTAB, water and oil, co-surfactant and surfactant at 0.6, 44, and 2, respectively. The micro-emulsion was prepared in two separate parts (A = 80% and B = 20% w/w). The A portion contained sulfur (37.8 mg) in oil phase and the B portion contained cadmium chloride (0.025 M) and ethylenediamine (0.41 M) in the aqueous phase of the micro-emulsion. The clear micro-emulsion of B was added slowly into the clear micro-emulsion of A and was irradiated with ultrasound (20 kHz Sonifier W-450, output acoustic power 45.5W, horn with 1.9 cm diameter) for 45 min in a given temperature (40ºC).

Absorption spectra. Absorption spectra were recorded by UV-Visible spectroscopy (Unico 2800). About 0.2 ml aliquots of the suspension were withdrawn at predetermined time intervals and diluted into micro-emulsion (4 ml). To quench any further reaction, the samples were immediately placed in ice water and stored under ice until the spectra were taken, usually within 20 min. A blank solution of micro-emulsion was used as the reference. Standard quartz cells with a 10 mm path-length were used and rinsed with micro-emulsion after each run. The experiments were performed in 45 min at 40, 48, and 60 ºC, respectively.

Sample Analysis. The structure and morphology of the final products have been studied in our recent work [23] by transmission electron microscopy (HRTEM, Hi-TEM is Hitachi 300 kV H-9500 TEM with accelerate voltage 100-300 kV and resolution 0.1 nm for the crystal lattice and 0.18 for point to point), and X-ray diffraction (XRD, the patterns were recorded in a wide angle range (2Θ = 10º-70º) by Bruker-axs, D8 Advance in scanning step of 0.02^{o}/sec, with monochromatized CuKα radiation λ = 1.5406 Aº).

RESULTS AND DISCUSSION

The results of optical, HRTEM and XRD measurements confirm that the size of nanoparticles are under 5 nm which means the formation of QDs [23]. The UV-Vis spectra of the samples at different interval times under constant temperature at 48 ºC are shown in Fig. 1. The absorbance onset is significantly blue-shifted from the value for the bulk of CdS which is about 515 nm (2.4 eV) and this is due to the quantum confinement of the particles [45].

By optical measurements, it is possible to determine the band gap which is sensitive to the presence of defects and contaminations. The optical absorption edge energies of crystalline species were obtained from UV-Vis absorption spectra. It is defined as the minimum photon energy required for exciting an electron from the top of the valence band to the bottom of the conduction band. In fact, the fundamental absorption is related to the band-to-band or to the exciton transition, that these transitions are classified according to the band structure of material, directly and indirectly [46]. Close to the absorption edge, the optical absorption coefficient (α) of the colloidal solution of QDs under Beer's law, is related to its band gap energy. This empirical relation is known as the Tauc-Lorentz plot (Eq. (1)) [47-49]:

$$(\alpha h\nu)^2 = \beta(h\nu - E^*) \quad (1)$$

where α is the absorption coefficient, β and E^* are constant and the band gap of the nanoparticle, respectively. The direct band gap can be estimated from the region where a steep increase of the adsorption was observed. In this region, band-to-band transition is characteristic and the particle band gap (E^*) can be determined by using Eq. (1) and extrapolating the linear portion of the plot to the energy axis at αhν = 0 (Figs. 2a, b, c) [50].

The value of the absorption coefficient can be calculated by Eq. (2) [49,51,52]:

$$\alpha = \frac{1}{d}\frac{-\log I_t/I_\circ}{\log e} = \frac{1}{d}\frac{A}{\log e} \quad (2)$$

where d is the thickness of the cuvette, I_t and I_o are the intensities of transmitted and incident light and A is the absorbance of the sample.

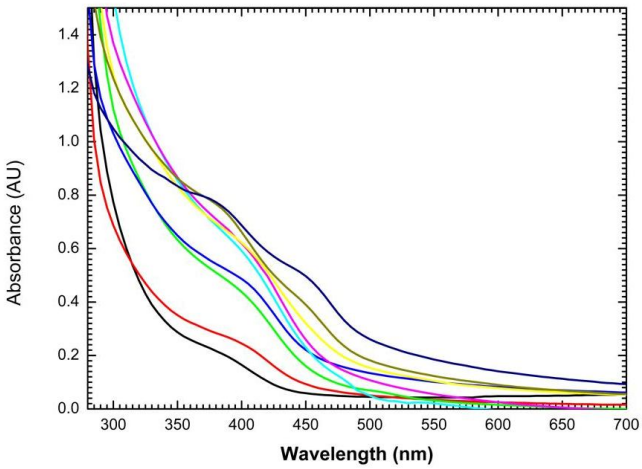

Fig. 1. The UV-Vis spectra of sample at different interval times at 48 ºC : 0.5 min, 2 min, 3 min, 5 min, 7 min, 10 min, 15 min, 30 min, 45 min.

Figure 2 shows that the band gap shifts to the lower energies very fast at the beginning of sonication and then changes with time slowly.

Growth Kinetics

To study the kinetics of the growth process, it is necessary to determine the particle size and particle size distribution as a function of time at different temperatures. In this study, two models have been used for estimating the nanoparticle size from band gap values: tight binding (TB) (Eq. (3)) [53] and the effective mass approximation (EMA) models [54].

$$E^* - E_g^{bulk} = \frac{1}{aD^2 + bD + c} \quad (3)$$

where E^* is the ban dgap of nanoparticle and E_g^{bulk} for a bulk. The constants of a, b, and c are 0.1278 nm^{-2} eV^{-1}, 0.1018 nm^{-1} eV^{-1}, and 0.1821 eV^{-1} for CdS, respevtively. D is the particle diameter [53].

For CdS nanoparticles with sizes less that 5 nm, the tight binding (TB) method has been shown a better fit to the experimental values [55]. However, in this work, Fig. 3 shows that the EMA method has a better fit for estimating

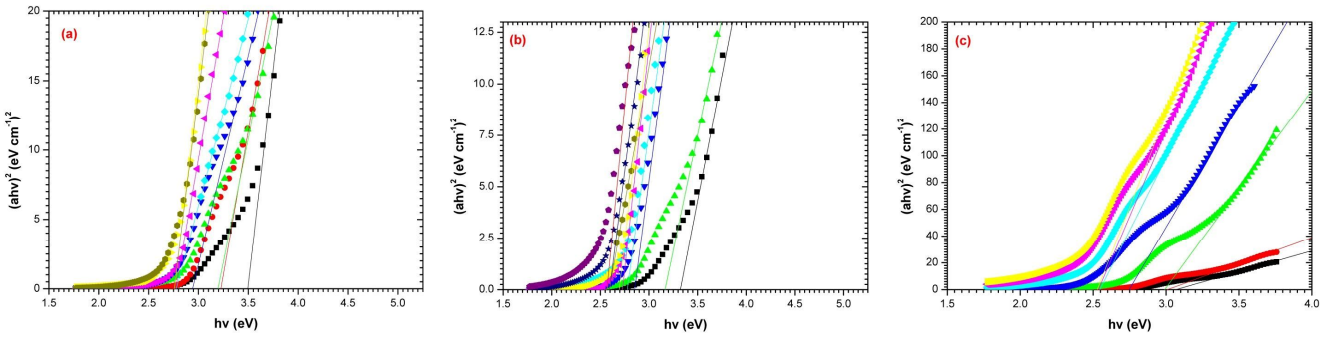

Fig. 2. Plot of $(\alpha h\nu)^2$ *vs*. (hν) at different temperatures: (a) 40 °C: ■ 0.5 min, ● 1 min, ▲ 2 min, ▼ 3 min, ◆ 7 min, ◀ 15 min, ▶ 30 min, ⬢ 45 min. (b) 48 °C: ■ 0.5 min, ▲ 2 min, ▼ 3 min, ◆ 5 min, ◀ 7 min, ▶ 10 min, ⬢ 15 min, ★ 30 min, ⬟ 45 min. (c) 60 °C: ■ 0.5 min, ● 1 min, ▲ 2 min, ▼ 5 min, ◆ 10 min, ◀ 30 min, ▶ 45 min.

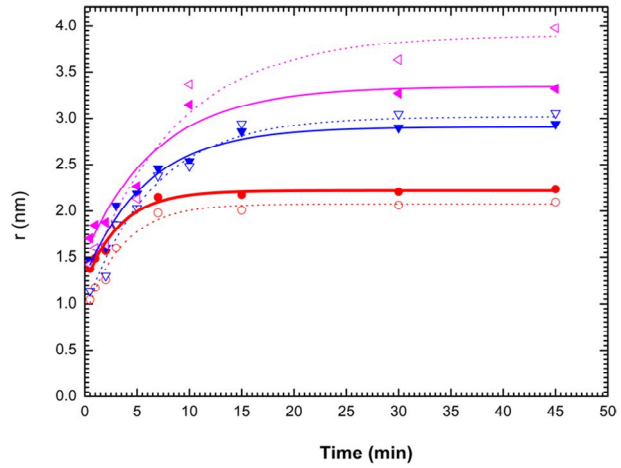

Fig. 3. Average particle radius *vs*. Time for the growth of CdS particles: tight binding (○ 40 °C, ▽ 48 °C, ◁ 60 °C)) and the effective mass model (● 40 °C, ▼ 48 °C, ◀ 60 °C).

the nanoparticle size with increasing temperature. In addition, a better agreement was observed between the size obtaind from the TEM images [23] and EMA than TB model. Therefore, in this study EMA model was selected for calculating the particle size (Eq. (4)).

$$E^* \cong E_g^{bulk} + \frac{h^2\pi^2}{2r^2}\left(\frac{1}{m_e^*} + \frac{1}{m_h^*}\right) - \frac{1.8e^2}{4\pi\varepsilon_0\varepsilon r} \qquad (4)$$

where E^* is the ban dgap of nanoparticle and E_g^{bulk} for the bulk, ħ = h/2π where h is the Planck's constant, r is the particle radius, m_e^* is the effective mass of electrons (0.19 m_e in CdS) , m_h^* is the effective mass of holes (0.8 m_e in CdS), e is the charge on an electron, ε_0 is the permittivity of free space, and ε is the relative permittivity. The simplified expression for the energy E^* in the case of CdS nanoparticles with radius r is shown in Eq. (5) (Eg = 2.4 eV, and ε = 5.7) [56]:

$$E^* \cong 2.4 + \frac{2.446}{r^2} - \frac{0.3031}{r} \qquad (5)$$

Figure 3 shows the time dependence of the average particle at different temperatures. It is clearly shown that the growth of the particles is dependent on temperature and time. In all cases, the size of nanocrystalline increases continuously with time. In addition, the particle size increases at any time with increasing the temperature. Based on Fig. 4, the red shift in the absorbance onset with time is related to the decrease in band gap associated with particle growth. The growth kinetics can be described and fitted by Ostwald Ripening (OR) model. After nucleation and growth, the particle size continues to further increase in size by coarsening model. This model involves the growth of larger crystals by the expense of smaller ones. For sufficiently large particles and by assuming diffusion-limited coarsening, the coarsening kinetics based on LSW model is given in Eq. (6) [35,36,33,39] and the plot are shown in Fig. 5.

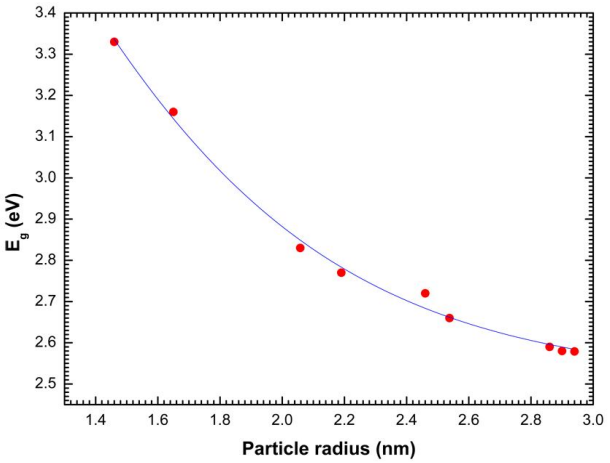

Fig. 4. Size dependence of the band gap for CdS nanoparticles at 48 ºC (particle radius from Eq. (4)).

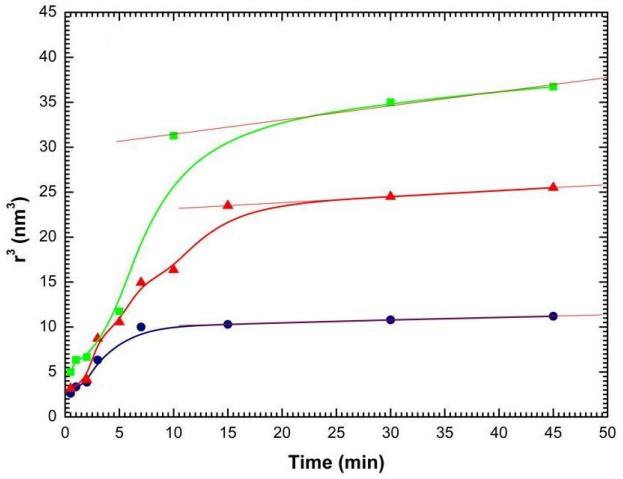

Fig. 5. LSW plot showing ripening of CdS quantum dots (results from Fig. 3 were replotted as r_{av}^3 *vs*. time) (● 40 ºC, ▲ 48 ºC , ■ 60 ºC.

$$r_{av}^3 - r_{\circ}^3 = kt \qquad (6)$$

where r_{av} is the average particle radius after ripening occurs, r_o is the average initial particle radius before ripening occurs, t is time and k is the ripening rate constant.

Figure 5 shows the growth based on the data from Fig. 3. It is replotted as r_{av}^3 *vs*. time at different temperatures. This figure shows the emergence of linear regions after about 15 min. This indicates an increase in particle size at longer times which is related to the diffusion-limited coarsening.

Evolution of Particle Size Distribution

The particle size distribution can be obtained from analysis of the absorption edge by taking the derivative of $A(r)$ with respect to the particle radius from (Eq. (7)) [26,34,43]:

$$n(r) \; \alpha \; - \frac{dA/dr}{\frac{4}{3}\pi r^3} \qquad (7)$$

where $n(r)$ and $A(r)$ are the particle size distribution and the absorbance, respectively. As the effective mass approximation can be used to connect the band gap to the particle radius (Eqs. (4) and (5)), it is possible to determine the particle size distribution from the absorption edge. In fact, the particle size distribution can be related to the local slope of the absorbance spectrum at the absorption edge. Hence, first the absorption edge is extracted from the absorption spectrum (the exciton peak). Next the wavelength axis of the absorbtion spectrum is converted to energy and then to radius using the effective mass approximation. Finally, a suitable fitting method is used to obtain the slope ($dA(r)/dr$) at each radius and then divided by the particle volume at that radius to obtain $n(r)$ [26,34,43].

Figure 6 shows the size distribution obtained from analysis of the absorption edge with the size distribution obtained from analysis of TEM images in the presence and absence ultrasound. In contrast to the classical method, there is a good agreement between the size obtained from analysis of the absorption edge and the TEM images in the presence of ultrasound. In the classical method, the absorbance edge is not clear which is due to the weak crystallite nanoparticles [23].

The maximum distribution obtained from analysis of the absorbance spectra can be considered as an average particle size. It is observed that in the presence of ultrasound, the maximum peak of the distribution is located at the size of

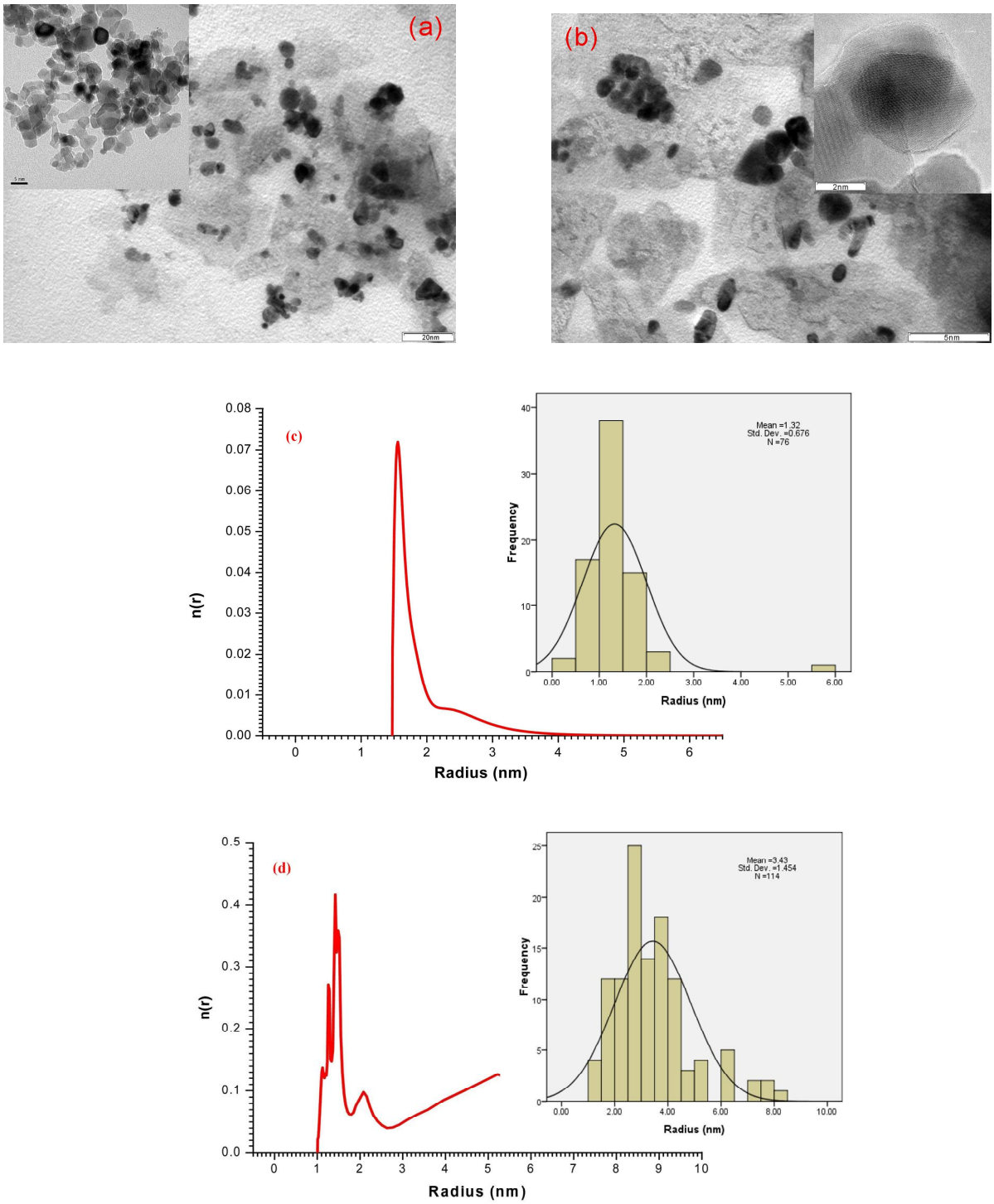

Fig. 6: TEM images of the prepared CdS: (a) stirring, 30 min (b) sonication, 30 min (Reprinted with permision from Ref. [23]. Copyright (2011) Elsivier), Size distribution histograms obtained from TEM images and size distributions calculated from absorbance spectra after 30 min of growth at 60 ºC, (c) ultrasound, (d) classical method.

1.55 nm, while the measurement of the size of the same nanoparticles from the transmission spectra results in 1.32 nm. In addition, the distributions obtained from the absorbance are sharper than those obtained from TEM images. This might be concerned to the difficulty in obtaining precise measurements of smaller particles from TEM images [26]. These measurements have shown a reasonable estimate of the particle size distribution for CdS QDs from analysis of the absorbance spectra.

Figure 7 shows the size distributions of the particles obtained from analysis of the absorbance spectra with time for nanocrystals at 60 ºC. The distributions appear relatively symmetrical with time and the radius at the maximum of distributions increases with time. Initially, a large number of particles nucleate and grow until the concentration of the solute dropps to the saturation level. The maximum peak is obtained at 5 min indicating that growth from supersaturation is completed at this time and coarsen at later times by Ostwald ripening.

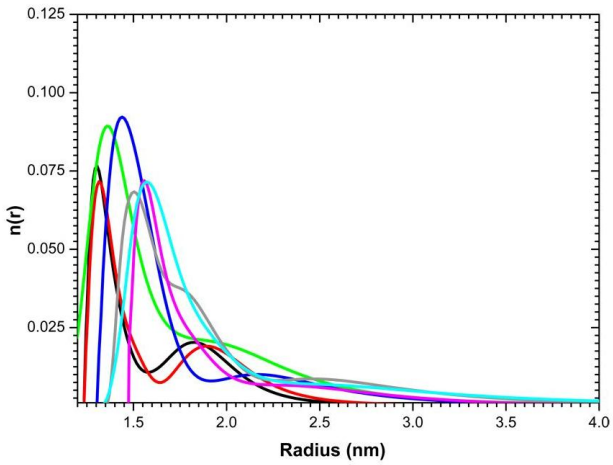

Fig. 7. Size distributions calculated from absorbance spectra with time at 60 ºC (Fig. 7 from ref. [23]), 0.5 min, 1 min, 2 min, 5 min, 10 min, 30 min, 45 min.

Activation Energy

The rate constant k can be obtained from the slopes of the linear regions of the plots of r_{av}^3 *vs*. time according to Eq. (6) at different temperatures and then uses for the kinetics analysis. The temperature dependence of the rate constant can be written as Eq. (8), the Arrhenius-type equation [2,26,39].

$$k = k_o \exp\left(-\frac{E_a}{RT}\right) \tag{8}$$

Here, k_0 is a constant and E_a is the activation energy for ripening. By obtaining the k values from LSW plot in Fig. 5, the Arrhenius plot can be obtained as shown in Fig. 8. From the slope of the line, the activation energy for the ripening was found to 71.72 kJ mol^{-1}. Hence, by substituting Eq. (8) into Eq. (6), the ripening kinetics can be rewritten as Eq. (9):

$$r_{av}^3 - r_o^3 = k_o \exp\left(-\frac{E_a}{RT}\right) t \tag{9}$$

The effect of temperature is an important factor on the nanoparticle's growth and the final size of the nanoparticles. An increase in temperature leads to a higher mass transfer

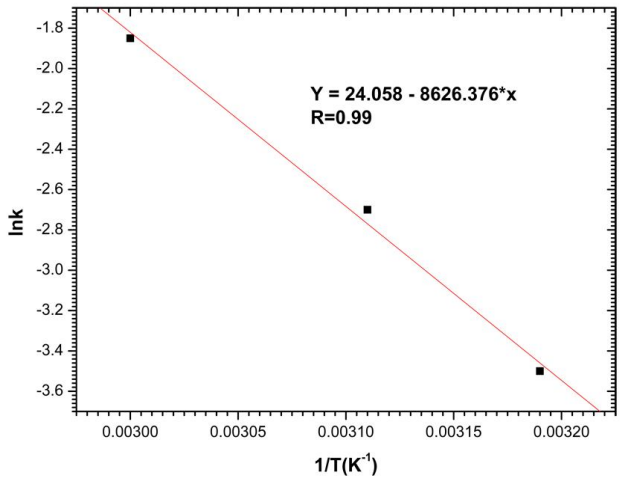

Fig. 8. Arrhenius plot of CdS nanocrystal quantum dots for the Ostwald ripening.

between two phases and enhances the growth rate. Additionally, acoustic cavitation produced by ultrasonic waves can strongly increase the mass transfer. Therefore, cavitatoin can increase the rate coarsening more than conventional methods [2,26,32,34].

CONCLUSIONS

Quantum dots of CdS with hexagonal phase have been prepared at relatively low temperature (60 ºC) and short time in micro-emulsion (O/W) under ultrasound. The nanoparticles have uniform spherical morphology with very small size (≈ 2 nm). The absorbance onset is significantly blue-shifted which is due to the quantum confinement of the particles. In this work, a detailed studies of the growth process under ultrasound are reported for the first time. It is clearly shown that the growth of the particles is dependent on temperature and time. The growth law for nanometer size of CdS particles is in consistent with Ostwald ripening kinetics model. The cubed average particle radius presents a linear region at longer times under different applied temperatures. This indicates that the increase of the particle size at longer times is related to the diffusion-limited coarsening. The rate constant for coarsening increases with temperature. Arrhenius-type plot was created by using the slopes of the LSW curves for the CdS nanocrystals and the activation energy for the ripening was evaluated to 71.72 kJ mol^{-1}. These results suggest that cavitatoin lowers the activation energy for the coarsening process. In fact, acoustic cavitation is responsible for mixing the phase reactions which increases the interfacial area and the mass transfer between two phases and therefore, the diffusion is rather easier under ultrasound than conventional method. Furthermore,the measurement results from analysis of the absorbance spectra have shown a reasonable estimate of the particle size distribution for CdS nanoparticles.The distributions appear relatively symmetrical with time and the radius at the maximum in the distributions increases with time.

ACKNOWLEDGMENTS

This work has been supported by the “Iranian National Science Foundation: INSF” (No. 85103/31).

REFERENCES

[1] P.V. Kamat, J. Phys. Chem. C 112 (2008) 18737.
[2] Y.-M. Sung, K.-S. Park, Y.-J. Lee, J. Phys. Chem. C 111(2007) 1239.
[3] N. Guijarro, T. Lana-Villarreal, I. Mora-Sero´, J. Bisquert, R. Gomez, J. Phys. Chem. C 113 (2009) 4208.
[4] Y. Liang, C. Zhen, D. Zou, D. Xu, J. Am. Chem. Soc. 126 (2004) 16338.
[5] J. Chen, X. Wang, Z. Zhang, Mater. Lett. 62 (2008) 787.
[6] S.Q. Sun, T. Li, Cryst. Growth Des. 7 (2007) 2367.
[7] G.Z. Shen, J.H. Cho, J.K. Yoo, G.C. Yi, C.J. Lee, J. Phys. Chem. B 109 (2005) 9294.
[8] S. Kundu, H. Lee, H. Liang, Inorg. Chem. 48 (2009) 121.
[9] M. Ethayaraja, K. Dutta, D. Muthukumaran, R. Bandyopadhyaya, Langmuir 23 (2007) 3418.
[10] R. Thiruvengadathan, Y. Levi-Kalisman, O. Regev, Ultrason. Sonochem. 14 (2007) 398.
[11] H.O. Wingkei, J.C. Yu, J. Mol. Catal. A: Chem. 247 (2006) 268.
[12] A. Tiehm, S. Krabnitzer, Y. Koltypin, A. Gedanken, Ultrason. Sonochem. 16 (2009) 617.
[13] R. Vijayakumar, Y. Koltypin, I. Felner, A. Gedanken, Mater. Sci. Eng. A 286 (2000) 101.
[14] J.H. Bang, W.H. Suh, K.S. Suslick, Chem. Mater. 20 (2008) 4033.
[15] D.J. Flannigan, K.S. Suslick, Nature 434 (2005) 52.
[16] K.S. Suslick, G.J. Price, Annu. Rev. Mater. Sci. 29 (1999) 295.
[17] M.M. Mdeleni, T. Hyeon, K.S. Suslick, J. Am. Chem. Soc. 120 (1998) 6189.
[18] K.S. Suslick, S.J. Doktycz, in: T.J.Mason (Ed.), Advances in Sonochemistry, Vol. 1, JAI Press, New York, 1990.
[19] S. Avivi (Levi), O. Palchik, V. Palchik, M.A. Slifkin, A.M. Weiss, A. Gedanken, Chem. Mater. 13 (2001) 2195.
[20] W. Guo, Z. Lin, X. Wang, G. Song, Microelectron. Eng. 66 (2003) 95.
[21] M.H. Entezari, N. Ghows, M. Chamsaz, J. Phys. Chem. A 109 (2005) 4638.
[22] S. Freitas, G. Hielscher, H.P. Merkle, B. Gander, Ultrason. Sonochem. 13 (2006) 76.
[23] M.H. Entezari, N. Ghows, Ultrason. Sonochem. 18 (2011) 127.
[24] N. Ghows, M.H. Entezari, Ultrason. Sonochem. 17

(2010) 878.
[25] F. Caruso, Colloids and Colloid Assemblies, Wiley-VCH Verlag GmbH & Co. KGaA, Weinheim, 2004.
[26] J. Park, K. Hyi Lee, J.F. Galloway, P.C. Searson, J. Phys. Chem. C 112 (2008) 17849.
[27] J.L. Zhao, J.A. Bardecker, A.M. Munro, M.S. Liu, Y.H. Niu, I.K. Ding, J.D. Luo, B.Q. Chen, A.K. Y. Jen, D.S. Ginger, Nano Lett. 6 (2006) 463.
[28] M. Bruchez, M. Moronne, P. Gin, S. Weiss, A.P. Alivisatos, Science 281 (1998) 2013.
[29] Y.J. Chan, S. Steckel, P.T. Snee, J.M. Caruge, J.M. Hodgkiss, D.G. Nocera, M.G. Bawendi, Blue Semiconductor Nanocrystal Laser, Appl. Phys. Lett. 86 (2005) 073102.
[30] J. Scha¨fer, J.P. Mondia, R. Sharma, Z.H. Lu, A.S. Susha, A.L. Rogach, L. Wang, Quantum Dot Microdrop Laser, Nano Lett. 8 (2008) 1709.
[31] L. Manna, E.C. Scher, A.P. Alivisatos, Synthesis of Soluble and Processable Rod-, Arrow-, Teardrop-, and Tetrapod-Shaped CdSe Nanocrystals, J. Am. Chem. Soc. 122 (2000) 12700.
[32] C.B. Murray, C.R. Kagan, M.G. Bawendi, Annu. ReV. Mater. Sci. 30 (2000) 545.
[33] G. Oskam, A. Nellore, R.L. Penn, P.C. Searson, J. Phys. Chem. B 107 (2003) 1734.
[34] Z. Hu, D.J. Escamilla Ramırez, B.E. Heredia Cervera, G. Oskam, P.C. Searson, J. Phys. Chem. B 109 (2005) 11209.
[35] I.M. Lifshitz, V.V. Slyozov, J. Phys. Chem. Solids 19 (1961) 35.
[36] C.Z. Wagner, Elektrochem. 65 (1961) 581.
[37] F. Huang, H.Z. Zhang, J.F. Banfield, J. Phys. Chem. B 107 (2003) 10470.
[38] T. He, D.R. Chen, X.L. Jiao, Chem. Mater. 16 (2004) 737.
[39] E.M. Wong, J.E. Bonevich, P.C. Searson, J. Phys. Chem. B 102 (1998) 7770.
[40] Z. Hu, G. Oskam, P.C. Searson, J. Colloid Interface Sci. 263 (2003) 454.
[41] E.M. Wong, P.G. Hoertz, [C.J. Liang, B.M. Shi, G.J. Meyer, P.C. Searson, Langmuir 17 (2001) 8362.
[42] Z.S. Hu, G. Oskam, R.L. Penn, N. Pesika, P.C. Searson, J. Phys. Chem. B 107 (2003) 3124.
[43] N.S. Pesika, K.J. Stebe, P.C. Searson, J. Phys. Chem. B 107 (2003) 10412.
[44] R.S.Yadav, P. Mishra, R. Mishra, M. Kumar, A.C. Pandey, Ultrason. Sonochem. 17 (2010)116).
[45] D. Jian, Q. Gao, Chem. Eng. J. 121
[46] R.A. Smith, (2nd ed.), Semiconductors, Cambridge University Press, Cambridge,
[47] J.M. Stillahn, K.J. Trevino, E.R. Fisher, ACS Appl. Mater. Interfaces 3 (2011) 1402.
[48] J. Tauc, R. Grigorovic, A. Vancu, Phys. Status Solidi 15 (1966) 627.
[49] M. Deepa, A. Kharkwal, A.G. Joshi, A.K. Srivastava, J. Phys. Chem. B 115 (2011) 7321.
[50] Y. Gao, Y. Masuda, H. Ohta, K. Koumoto, Chem. Mater 16 (2004) 2615.
[51] P.H.T. Ngamou, N. Bahlawane, Chem. Mater. 22 (2010) 4158.
[52] R. Brahimi, Y. Bessekhouad, A. Bouguelia, M. Trari, J. Photochem. Photobiol. A: Chem. 194 (2008) 173.
[53] C.N.R. Rao, A. Muller, A.K. Cheetham, Nanomaterial Chemistry, Wiley-VCH Verlag GmbH & Co. KGaA, Weinheim, 2007.
[54] L. Brus, J. Chem. Phys. 80 (1984) 4403.
[55] P.E. Lippens, M. Lanno, Phys. Rev. B 39 (1989) 10935.
[56] S.S. Shiv, C. Sayandev, S. Murali, Phys. Chem. Commun. 6 (2003) 36.